



# Application of Morphometric Ranking Approach using Geospatial Techniques for Flash Flood Susceptibility Modelling in District Shangla, Pakistan

Muhammad Akmal Sardar Ali<sup>1,2</sup>, Abid Sarwar<sup>1,2\*</sup>, Muhammad Ali<sup>2</sup>, Shazia Gulzar<sup>1,2</sup>, Abdul Majid<sup>1</sup>, Muhammad Ismail Khan<sup>1</sup>, Jabir Nazir<sup>2</sup>, and Arbaz Ahmad<sup>3</sup>

<sup>1</sup>Directorate General Soil & Water Conservation, Peshawar, Pakistan

<sup>2</sup>National Centre of Excellence in Geology, University of Peshawar, Pakistan

<sup>3</sup>Department of Geography and Geomatics, University of Peshawar, Pakistan

**Abstract:** Every year, disaster strikes, and led to thousands of casualties and deaths around the world. A meteorological disaster such as a flash flood is a multifaceted hydro-meteorological phenomenon that can cause a huge loss of human life and can create severe economic problems. In this study, techniques based on Geographic information systems and Remote sensing were used to get the flood susceptibility map for District Shangla, Pakistan. For the susceptibility of flash floods, geo-morphometric ranking model was used. Various causative factors were considered including; topography, river pattern, and flow accumulation. ALOS PALSAR digital elevation model was used for calculating the required causative factors. Eleven different sub-basins were delineated in the Shangla basin. A total of eighteen morphometric parameters were studied. The morphometric ranking approach (MRA) score was determined with a range of 1 to 5. Rank 5 represents high risk while rank 1 exhibits low risk. The results of the model were categorized into five flood vulnerability classes; very low, low, moderate, high and very high. The total population of Shangla district is 757,810 with a population density of 480 persons per sq km<sup>2</sup>, and results from this study revealed that 23% of the total geographic area (364.11 km<sup>2</sup>) of the district is vulnerable to high flash floods.

**Keywords:** Geo-morphometric, GIS, Remote Sensing, Susceptibility, Vulnerability, Flash flood

## 1. INTRODUCTION

Every year, disaster strikes, and led to thousands of casualties and deaths around the world [1, 2]. According to estimates, hydrological and climatological disasters have produced extensive damage to individuals and infrastructure [3, 4]. One of the most devastating hydrometeorological disasters is flooding [5-7]. More than one-third of the earth's land surface inhabited by over 70 % of the world's population is prone to floods [8]. It has been observed that floods are mainly caused by heavy rainfall, changes in terrain and glaciers melting [9]. It is obvious that there is a possibility that the rainfall will increase, which may lead to an increase in destructive flooding in the future [10, 11]. A meteorological disaster such as a flash flood is

a multifaceted hydro-meteorological phenomenon which can cause huge losses to human lives and can create severe economic problems [12]. Flash floods constantly occur without any early warning system or form of forecasting [13], especially in Pakistan. Heavy and persistent rain increases river and stream discharge, which leads to severe flash floods [14]. Flash floods are local wonders which always occur in basins having area of a few square kilometers with a very short reaction time [15]. Uneven and unstable land surfaces can also increase surface flow and abruptly decrease the reaction time to a flash flood event [16]. Hu discovered that the geomorphometric characteristics of the basin and climatic conditions are the main triggering factors for flash floods [17]. The high peak discharge from flash floods bring the human life and urban

structure at more risk [18]. Different factors which lead to flash floods are high and heavy rainfall, the topography of watershed, land cover/land use, permeability of soil, soil texture and natural susceptibility [19-20]. Flash floods are considered as the most devastating hydrological hazard because of their abrupt and unpredictable character, the extensive harm they wreak, and the hazards they bring to physical infrastructure and livelihoods [21-24]. Two of the key factors that determine the likelihood of flash floods are volume and intensity of precipitation [25].

Additional interconnected factors responsible for overall intensity of flash floods include evaporation, the characteristics of the river system, catchment size, natural and anthropogenic activities within the basins. [26]. Watershed's geomorphic structures are of utmost importance for evaluating and controlling extreme hydrological phenomena like flash floods. The structure and shape of a watershed are measured mathematically using morphometry. Stream order, stream number, stream length, stream density, drainage frequency, watershed size, perimeter, shape factor, and circulatory ratio are some of the basin variables that are numerically analyzed in morphometry [27-30].

Many researchers performed significant research on basin characterization morphometry [31]. Mapping the earth's surface morphology is helpful to analyze geological, hydrological/groundwater conditions to prevent soil erosion [32-35] and modeling of flash flood vulnerability [36-39]. Geological, geomorphological, and hydrometeorological characteristics of a basin/watershed are responsible factors for controlling the drainage geometry and density [40, 41]. Until recently, fieldwork, topographical maps and aerial photography were employed to determine the boundaries of drainage networks. Most recently, geographic information systems and remote sensing are often employed for morphometry and drainage system delineation [42-46]. Flash flood susceptibility modelling uses geospatial approaches, which are robust, time- and capital-saving tools for processing, mapping, and evaluating of watersheds [47-50]. Various studies (especially those cited in this manuscript), have applied Morphometric analysis for watershed assessment and flash flood susceptibility modelling [51, 52].

In morphometric analysis, mathematical and quantitative analysis is carried out in order to understand the correlation of flow patterns and terrain characteristics with the geohydrological features of a hydrological domain. Morphometric parameters (MPs) obtained from remotely sensed data collected are effective, precise, and cost- and time-effective input data for forecasting flash flood susceptibility. Numerous hydrological disasters, such as flash floods, can either be mitigated or avoided with the use of geospatial approaches, which can evaluate the hydrological response at the watershed level [53, 54]. To lessen the danger posed by the flash flood, it is crucial to identify watershed flash flood potentiality [55]. Mohamed and El-Raey [56] employed MPs to assess the flash flood vulnerability in Southeast Bangladesh. The study found that remote sensing data in integration with GIS considerably improved comprehension of flash floods, and assisted in reducing their consequences on property destruction and financial losses. Researchers have found that using the GIS ArcHydro tool to extract properties from a DEM and automatically demarcating topographic and morphometric features is a suitable alternative to manually reviewing topographic maps and conducting field research [57-58].

The primary goal of the current study is to locate the most vulnerable places to flash floods as well as the key flash flood-prone zones in the study area.. Like the rest of Pakistan, the Shangla basin's physiography and climate make it particularly susceptible to flash floods. In monsoon, due to intense rainfall and heavy melting of snow on surrounding mountains, the area is facing frequent flash floods. The current study will offer an avenue for research and knowledge to lessen the devastating consequences of flash floods in the study area.

## **2. MATERIALS AND METHODS**

### **2.1. Study Area**

This research focused on the district Shangla, Khyber Pakhtunkhwa, Pakistan. District Shangla lies between 34° 31' to 35° 01' north latitude and 72° 33' to 73° 01' east Longitude. The total geographical area is 1586 square kilometers with 36 % cultivated and 64 % of forest area. The district's landscape is dominated by tall mountains and small valleys

in the western Himalayas. The district is generally between 2000 and 3500 meters above mean sea level. Figure 1 shows the study area.

**2.2 Data Collection**

Primary sources in addition to secondary data sources were utilized for achieving the mentioned aims. A physical visit to district Shangla was arranged to collect all the records of damages that occurred due to severe flood phenomena occurred in the past. The precipitation statistics were obtained from the Pakistan Meteorological Department (PMD), Islamabad. The irrigation department of Khyber Pakhtunkhwa facilitated net cashing information on the river. Lithological layers of the study area were acquired from the regional office of the Geological Survey of Pakistan (GSP). The ground particles consistency layer was extracted from the Directorate of Soil Survey, Khyber Pakhtunkhwa. Topographical information on the ground surface was extracted from high spatial resolution ALOS PALSAR DEM. Land use/cover patterns of the study area were derived for the year 2021 using freely available Landsat 8 satellite. Figure 2 shows the input data maps,

while definitions and mathematical calculations of various linear and aerial morphometric parameters are displayed in Table 1.

Identification of maximum (X-Max) and Minimum (X-MIN) risk values for the morphometric parameters is shown in Table 2. The formula below was used to calculate the minimum and maximum risk values.

$$Risk\ value = 4x\ X - X\ min / Xmax - Xmin$$

$$Risk\ value = 4x\ X - X\ max / Xmin - Xmax$$

X shows the variable value, Xmax denotes the extreme value and Xmin denotes the slightest value in the variables group.

Systemized variables were considered which contemplate the measured risk for each Morphometric variable in contrast with the equal variable lying in each sub-vessel. MRA grade estimated ranked between 1 to 5. Score 5 indicates a high flash flood risk and a score 1 indicates the least risk. The calculated ranking scores are shown in Table 3. In the final step, all the variables of each sub-vessel were added, followed by categorizing

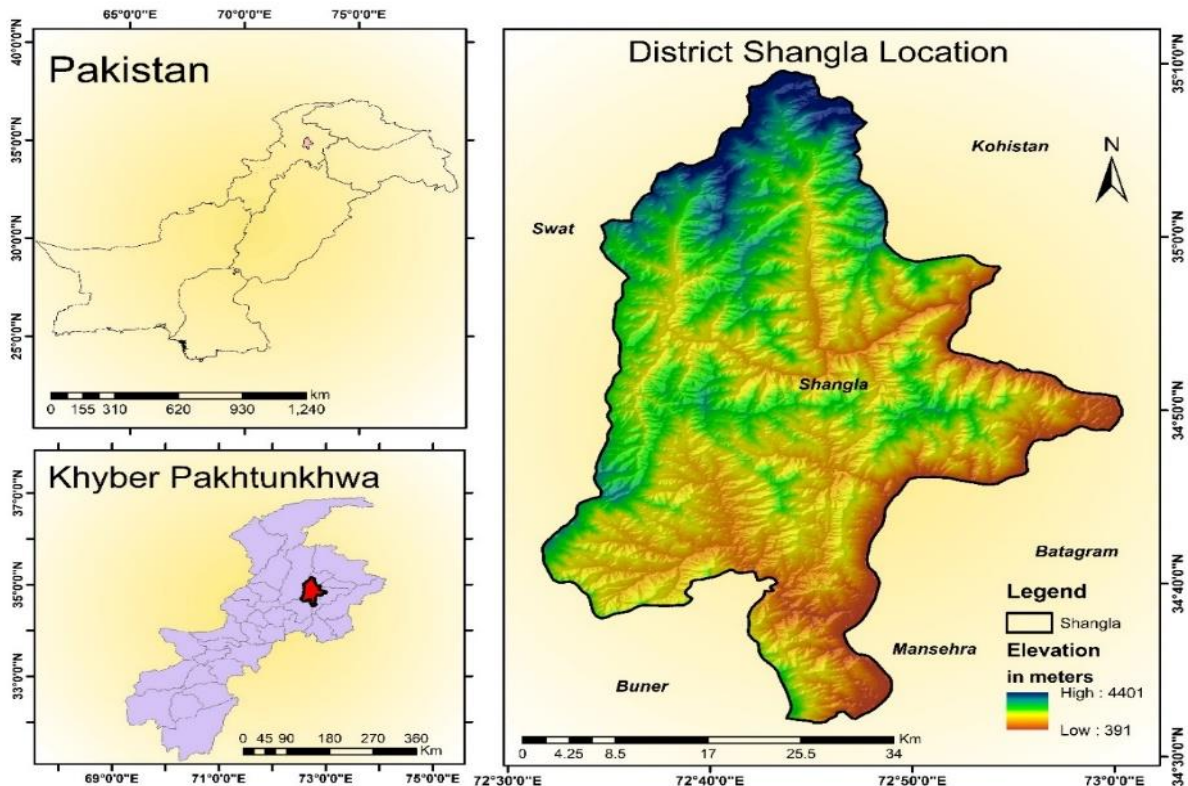


Fig. 1. The Study Area Map

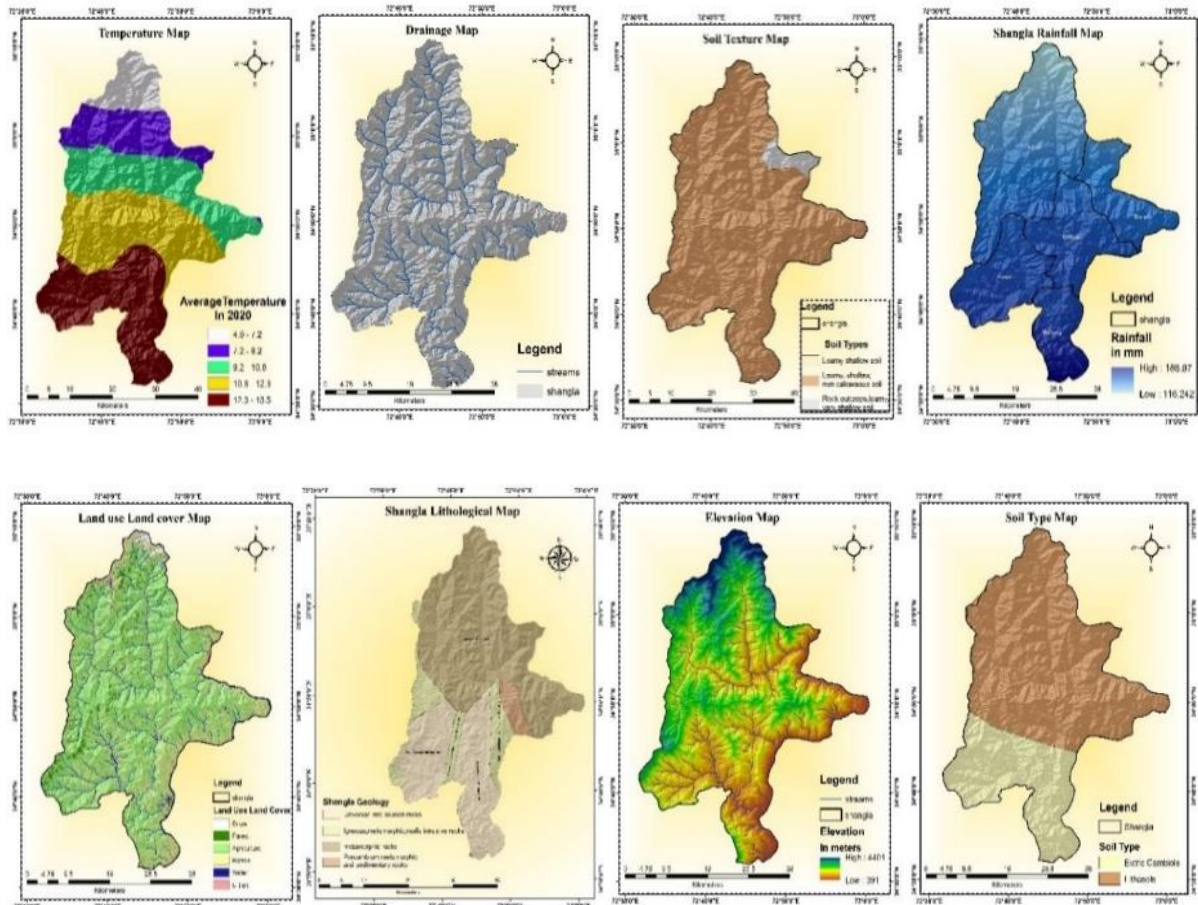


Fig. 2. District Shangla Input Data Maps

them into five groups. i.e. very high, high, moderate, low, and very low flooding susceptibility. Figure 3 shows the methodology flow chart.

### 3. RESULTS

Eleven (11) sub-basins were delineated in the study area, where eighteen geo-morphometric parameters for each sub-basin were analyzed and computed. For linear, aerial, and shape aspects of all sub-basins, a quantitative geo-morphometric analysis was carried out. The morphometric features reveal that there are some variations in different characteristics of each sub-basin (Table 2). Results reveal that area-wise, Sb-2 (sub-basin) is the smallest sub-basin covering an area of 30.64 km<sup>2</sup> and Sb-4 is the largest by area of 153.88 km<sup>2</sup> (Table 2).

According to geomorphology, the relief, gradient, type of rocks, and geologic formations in a drainage region, all influence the drainage flow pattern in a particular basin. Stream order 4<sup>th</sup> was

found to be the highest and stream order 2<sup>nd</sup> was the lowest in stream order (Table 2). Maximum of the sub-basins was delineated using stream order 3<sup>rd</sup> and stream order 4<sup>th</sup>. Figure 4a shows the stream order map of the sub-basins of the study area. The numbers represent the total number of streams that drain the basin. The lithology, soil properties, and rainfall patterns of the basin affect the number of streams. The immediate discharge can be greatly increased by a higher stream number ( $S_n$ ). The Sb-4 is the sub-basin with the most streams (48), while Sb-2 has the fewest streams (9) (Table 2). Figure 4b shows the number of streams in sub-basins of the study area. Stream length ( $L_u$ ) is considered one of the basin's most important hydrological qualities as it exposes information about surface runoff. The Sb-4 has the highest length of stream (79.27 km) and Sb-2 has the lowest (14.71 km) (Figure 4c & Table 2). The stream frequency ( $F_s$ ) values are from 0.25 (Sb-1) to 0.38 (Sb-9) (Table 2). High relief and an impervious surface are indicated by the larger number of streams and stream frequency. The

**Table 1.** Morphometric Parameters and their Mathematical Formulas

Factor	Formula	Reference
Area (A) (km <sup>2</sup> )	A=area of basin	[59]
Length (L <sub>b</sub> )	L <sub>b</sub> = length of basin	[59]
Perimeter (P) (km)	P = Parameter of basin	[59]
Stream order (S <sub>o</sub> )	Ranking of stream	[60]
Number of stream (S <sub>n</sub> )	S <sub>n</sub> = N1 + N2 +.. ..... + Nn	[59]
Stream length (L <sub>u</sub> )	L <sub>u</sub> = L1 + L2. . . . . + Lu	[60]
Stream frequency (F <sub>s</sub> )	F <sub>s</sub> = S <sub>n</sub> / A	[59]
Drainage density (D <sub>d</sub> )	D <sub>d</sub> = L <sub>u</sub> / A	[59]
Relief (B <sub>h</sub> ) (m)	B <sub>h</sub> = h <sub>max</sub> - h <sub>min</sub>	[61]
Relief ratio (R <sub>r</sub> )	R <sub>r</sub> = B <sub>h</sub> / L <sub>b</sub>	[61]
Gradient (G)	G =B <sub>h</sub> / L <sub>b</sub> X 60	[62]
Circulatory ratio (C <sub>r</sub> )	C <sub>r</sub> = 4π A / P <sup>2</sup>	[60]
Elongation ratio (E <sub>r</sub> )	E <sub>r</sub> = 1.128 A <sup>(1/4)</sup> / L <sub>b</sub>	[61]
Shape factor (B <sub>s</sub> )	B <sub>s</sub> = L <sub>b</sub> <sup>2</sup> / A	[59]
Length of overland flow (L <sub>o</sub> )	L <sub>o</sub> =0.5 X 1/D <sub>d</sub>	[59]
Ruggedness number (R <sub>n</sub> )	R <sub>n</sub> = D <sub>d</sub> X (B <sub>h</sub> /1000)	[60]
Geomatery number (G <sub>n</sub> )	G <sub>n</sub> = B <sub>h</sub> X D <sub>d</sub> / G	[60]
Compactness coefficient (C <sub>c</sub> )	C <sub>c</sub> =0.2812 X P/A <sup>0.5</sup>	[59]

frequency of the sub-basins is shown in Figure 4d. Drainage density (D<sub>d</sub>) values are between 0.44 km/km<sup>2</sup> (Sb-3) and 0.53 km/km<sup>2</sup> (Sb-11). The drainage density in all sub-basins is more than 0.44 km/km<sup>2</sup> (Table 2 & Figure 5e). Sub-basin relief (B<sub>h</sub>) ranges from 1.6 meters (Sb-11) to 2.68 meters (Sb-1) (Table 2 & Figure 5f). The relief ratio (R<sub>r</sub>) of sub-basins is ranging from 0.10. (Sb-5) to 0.25 (Sb-2) (Table 2 & Figure 5g). The other important parameter is gradient which is derived from relief divided by the length of the basin (L<sub>b</sub>) multiplied by 60. The gradient values range from 6.44 (Sb-10) to 15.27 (Sb-2) (Table 2 & Figure 5h).

All sub-basins had elongation ratio (E<sub>r</sub>) values that were less than one, with the highest and lowest values ranging from 0.29 for Sb-2 to 0.17 for Sb-4 (Table 2 & Figure 6i). The values of shape factor

(B<sub>s</sub>) ranges from 2.74 to 3.41 (Table 2 & Figure 6j). The geometry number (G<sub>n</sub>) of the sub-basins ranges from 0.07 to 0.20 (Table 2 & Figure 6k). The ratio of the basin's size to its perimeter is known as the compactness coefficient (C<sub>c</sub>). The Sb-2 got the lowest C<sub>c</sub> value of 1.19 and Sb-11 got highest C<sub>c</sub> value of 1.66 (Table 2 & Figure 6l). The perimeter (P) of Sb-2 is showing lowest value equal to 23.36, and Sb-4 is having the highest value equal to 58.93 (Table 2 & Figure 7m). Circularity ratios (R<sub>c</sub>) with a value of more than 0.5 are present in more than half of the sub-basins (Table 2 & Figure 7n). Sb-2 had the highest R<sub>c</sub> score (0.70). As flood hazard levels are growing in proportion to the circularity ratio's magnitude, more than half of the sub-basin are at high risk from flood hazard. Ruggedness number (R<sub>n</sub>) is lowest in Sb-7 (0.0007) and highest in Sb-4 (0.0013) (Table 2 & Figure 7o). Length

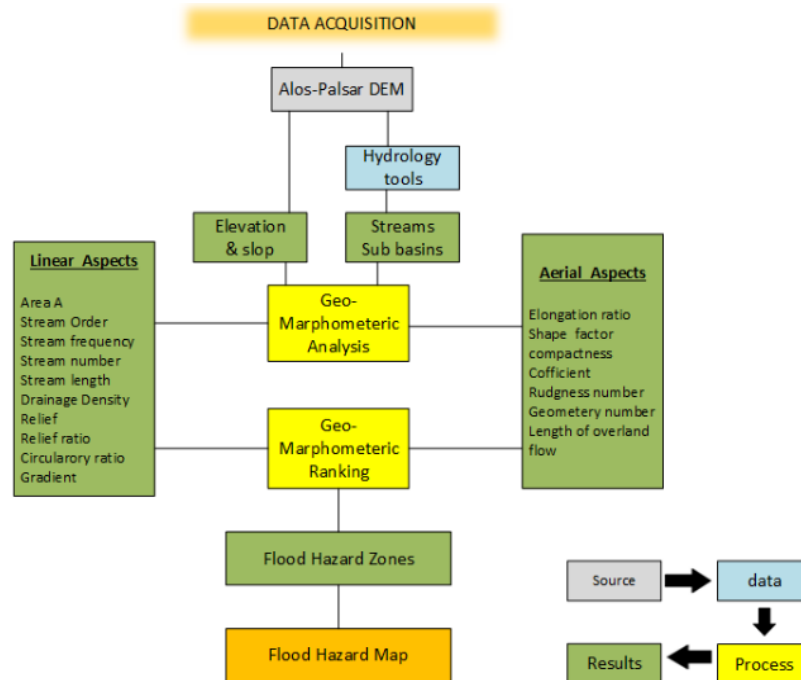


Fig. 3. Flow chart.

of the overland flow ( $L_o$ ) is the reciprocal of the drainage density. Sb-3 exhibits a high  $L_o$  value while Sb-11 has the lowest  $L_o$  value (Table 2 & Figure 8p). The period of concentration and size of the peak discharge at the basin outflow is directly impacted by the basin shape factor ( $B_s$ ). In comparison to an elongated basin with the same surface area, a circular basin will produce high discharge more quickly. Low values of the basin shape factor show a circular basin, whereas large values show an extended basin form. The lowest  $B_s$  value were observed for Sb-2 (2.74) (Table 2 & Figure 8q).

#### 4. DISCUSSION

According to the current study, Shangla is divided into 11 sub-basins with various geo-morphometric and physical properties. The upper range of the sub-basins represents snow-covered peaks and narrow valleys. Usually, a flash flood is caused by the monsoon rainfall. The melting of snow is accelerated in these seasons due to the heavy rainfall and high temperature above 32 °C, this results in flash floods in the upper ranges and riverine floods without prior warning in the lower ranges, and cause damages and disastrous effects throughout the basin.

#### 5.1 Flash Flood Hazard Zonation

The zones are further divided into very low, low, moderate, high, and very high zones and apply the geo-morphometric ranking approach. The nasscore of 1 to 5 were assigned to each geo-morphometric parameter of each basin. The geo-morphometric ranking number (GRN) was aggregated for each sub-basin ranked score to represent the hazards degree of flash flood hazard. The higher GRN score will represent a higher degree of flash flood hazard and vice versa. The range of GRN for all sub-basins is 39.18 to 55.14 (Table 3).

##### 4.1.1. Very High Flash Flood Hazard Zone

Geo-morphometric ranking model analysis in the study region reveals that 23 % (364.11 km<sup>2</sup>) of the region is marked as a very high hazard zone with respect to flash flood hazards in the Shangla basin (Figure 9). The very high hazard zone is categorized by the highest GRN (>51.41) which is shown by Sb-4, Sb-9, and Sb-10 (Table 3, & Figure 10). This zone remains highly vulnerable for the local people where the frequency of flash flood is very high. The dry channels are activated by the heavy rainfall in the months of June to August and cause flash floods. Steep slope of the channel causes high-speed flash

Table 2. Geo-Morphometric Characteristics of Sub Basins

zSub basin	A	P	L <sub>b</sub>	S <sub>0</sub>	S <sub>n</sub>	L <sub>u</sub>	F <sub>s</sub>	D <sub>d</sub>	B <sub>h</sub>	R <sub>r</sub>	G	C <sub>r</sub>	E <sub>r</sub>	B <sub>s</sub>	L <sub>o</sub>	R <sub>n</sub>	G <sub>n</sub>	C <sub>c</sub>
Sb-1	71.38	38.12	14.82	2	18	34.28	0.25	0.48	2.683	0.18	10.86	0.62	0.22	3.08	1.04	0.001288686	0.12	1.27
Sb-2	30.64	23.36	9.16	3	9	14.71	0.29	0.48	2.333	0.25	15.27	0.70	0.29	2.74	1.04	0.001120007	0.07	1.19
Sb-3	132.86	56.72	21.09	3	37	59.04	0.28	0.44	2.622	0.12	7.46	0.52	0.18	3.35	1.13	0.001165205	0.16	1.38
Sb-4	153.88	58.93	22.92	3	48	79.27	0.31	0.52	2.563	0.11	6.71	0.56	0.17	3.41	0.97	0.001320378	0.20	1.34
Sb-5	113.65	54.70	19.30	3	33	55.52	0.29	0.49	1.866	0.10	5.80	0.48	0.19	3.28	1.02	0.000911539	0.16	1.44
Sb-6	100.48	58.80	17.99	4	27	48.64	0.27	0.48	2.439	0.14	8.13	0.36	0.20	3.22	1.03	0.001180559	0.15	1.65
Sb-7	64.84	45.02	14.03	2	23	31.58	0.35	0.49	1.512	0.11	6.47	0.40	0.23	3.04	1.03	0.000736318	0.11	1.57
Sb-8	115.27	52.91	19.45	4	33	57.85	0.29	0.50	2.206	0.11	6.80	0.52	0.19	3.28	1.00	0.001107048	0.16	1.39
Sb-9	91.62	44.46	17.07	3	35	46.87	0.38	0.51	1.9	0.11	6.68	0.58	0.20	3.18	0.98	0.000971982	0.15	1.31
Sb-10	118.61	47.00	19.77	4	35	56.85	0.30	0.48	2.123	0.11	6.44	0.67	0.19	3.30	1.04	0.00101754	0.16	1.21
Sb-11	64.73	47.53	14.02	3	19	34.61	0.29	0.53	1.672	0.12	7.16	0.36	0.23	3.04	0.94	0.000893967	0.12	1.66

Table 3. Geo-morphometric Ranking

Sub basin	A	S <sub>0</sub>	S <sub>n</sub>	L <sub>b</sub>	F <sub>s</sub>	D <sub>d</sub>	B <sub>h</sub>	R <sub>r</sub>	G	C <sub>r</sub>	E <sub>r</sub>	B <sub>s</sub>	L <sub>o</sub>	R <sub>u</sub>	G <sub>n</sub>	C <sub>c</sub>	Ranking
Sb-1	2.32	1	1.92	2.25	1.00	2.78	5.00	3.00	3.14	4.06	3.33	2.97	1.32	1.22	4.99	4.32	44.62
Sb-2	1.00	3	1.00	1.03	2.23	2.78	3.80	5.00	5.00	5.00	1.00	5.00	1.32	2.37	5.00	5.00	49.53
Sb-3	4.32	3	3.87	3.78	1.92	1.00	4.79	1.29	1.70	2.88	4.67	1.36	1.00	2.06	4.98	3.38	46.00
Sb-4	5.00	3	5.00	5.03	2.85	4.56	4.59	1.00	1.38	3.35	5.00	1.00	3.75	1	4.91	3.72	55.14
Sb-5	3.69	3	3.46	3.56	2.23	3.22	2.21	0.71	1.00	2.41	4.33	1.78	4.29	3.8	4.87	2.87	47.43
Sb-6	3.27	5	2.85	3.14	1.62	2.78	4.17	1.86	1.98	1.00	4.00	2.13	4.61	1.96	4.77	1.09	46.23
Sb-7	2.11	1	2.44	2.08	4.08	3.22	1.00	1.00	1.28	1.47	3.00	3.21	4.82	5	4.66	1.77	42.14
Sb-8	3.75	5	3.46	3.71	2.23	3.67	3.37	1.00	1.42	2.88	4.33	1.78	4.93	2.46	4.12	3.30	51.41
Sb-9	2.98	3	3.67	3.03	5.00	4.11	2.33	1.00	1.37	3.59	4.00	2.37	4.96	3.39	3.57	3.98	52.35
Sb-10	3.86	5	3.67	3.64	2.54	2.78	3.09	1.00	1.27	4.65	4.33	1.66	5.00	3.07	1.93	4.83	52.32
Sb-11	2.11	3	2.03	2.27	2.23	5.00	1.55	1.29	1.57	1.00	3.00	3.21	5.00	3.92	1.00	1.00	39.18

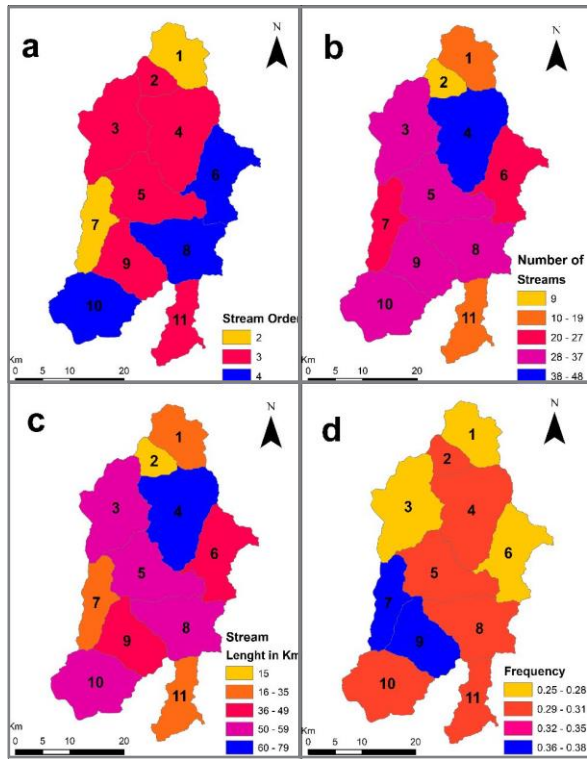


Fig. 4. District Shangla showing a. Stream order, b. Stream No, c. Stream Length, d. frequency.

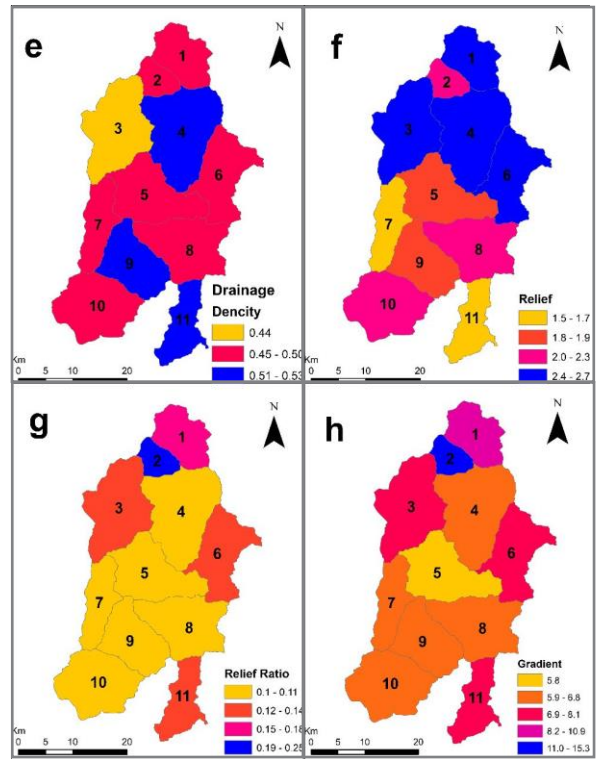


Fig. 5. District Shangla showing e. Drainage density, f. Relief, g. Relief ratio, h. Gradient.

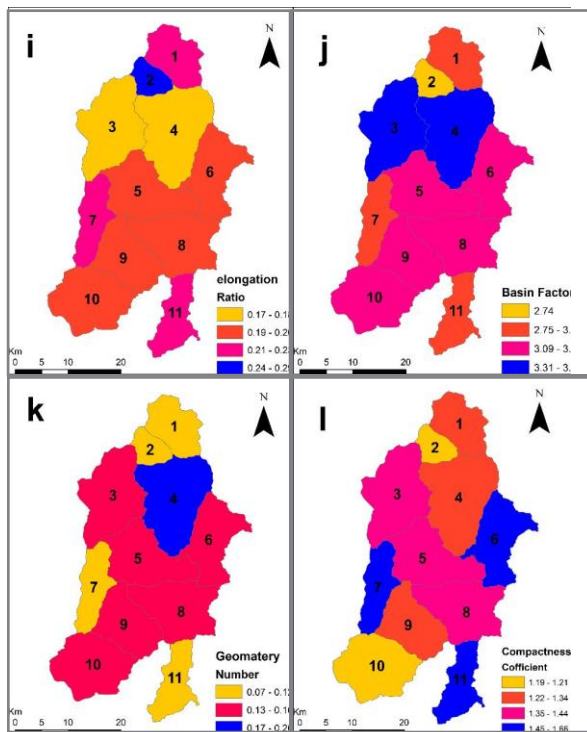


Fig. 6. District Shangla showing i. elongation ratio, j. Basin factor, k. Geometry Number, l. Compactness coefficient.

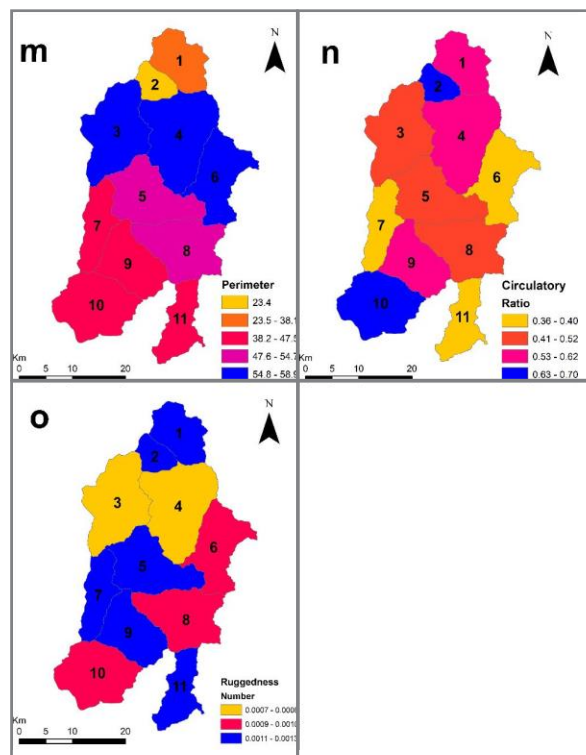
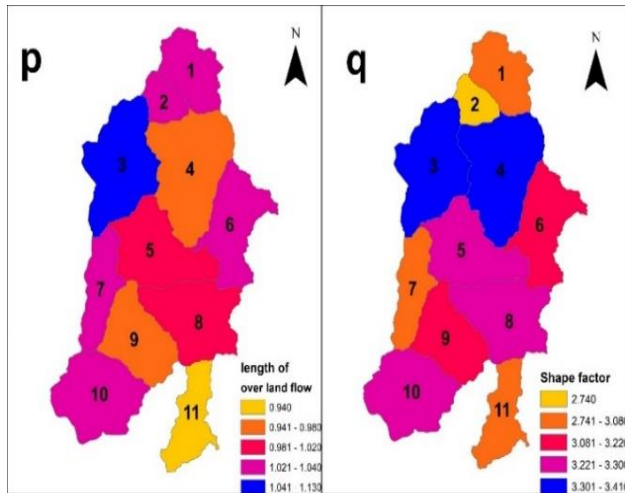


Fig. 7. District Shangla showing m. perimeter, n. circulatory ratio, o. Ruggedness Number.



**Fig. 8.** District Shangla showing p. length of overland flow, q. Shape factor

flood flow.

#### 4.1.2. High Flash Flood Hazard Zone

Results from the current study revealed that 9 % (145.89 km<sup>2</sup>) of the study area is mapped as a high-hazard zone for flash floods (Figure 9). Thus collectively, the total area under high to very-high hazard zone for flash floods is about 32 % of the study region. The high hazard zone was marked by ranking number (GRN) value ranges from 47.4 to 51.4 which are exhibited by Sb-2 and Sb-8 (Table 3, & Figure 10).

#### 4.1.3. Moderate Flash Flood Hazard Zone

The moderate flash flood hazard zone of the study region accounts for 7 % (113.65 km<sup>2</sup>) of the region (Figure 9). The moderate hazard zone was categorized by the geo-morphometric ranking number (GRN) value ranging from 46.23 to 47.43 as shown by Sb-5 (Table 3, & Figure 10). This basin has 3rd number of stream order and hence flood frequency is considered as a medium.

#### 4.1.4. Very Low to Low Flash Flood Hazard Zone

In the Shangla Basin, 61 % (1026.27 km<sup>2</sup>) has very low to low hazard of flash floods. It was also verified in the field that this zone is not experiencing a flood.

## 5. CONCLUSION

This study concludes that the morphometric analysis is a crucial tool for understanding flow patterns and

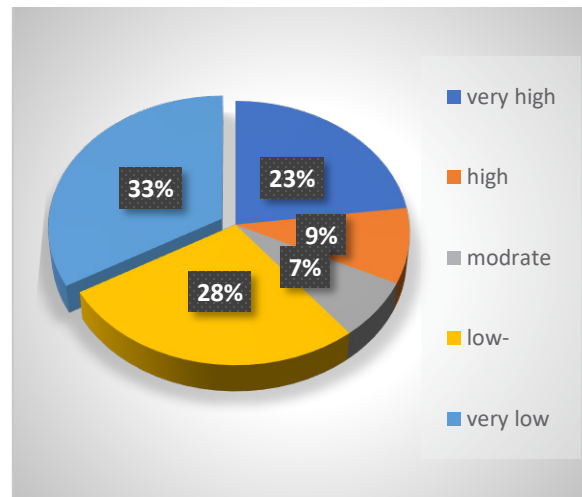


**Fig. 9.** Percentage of the area covered by flash flood hazard zones

its effects on the surrounding area. Such studies could be used for better planning, designing, and management of floodwaters (dams, embankments, protective walls, spurs etc.). Flood risks can be mitigated by designing a flood defence system based on the results derived from morphometric analysis. The morphometric analysis carried out in this study are helpful for risk modeling in order to establish link between flow pattern and terrain characteristics. Such modeling is an important factor in determining how risk will shift over time in response to varying pattern of different environmental variables. The engineering design of dams, bridges, culverts, and flood control structures are only a few examples of the various engineering applications for which the flood morphometric analysis can be utilized. Additionally, it can be used to delineate floodplains, determine human activity within floodplains, and estimate the financial benefits of flood mitigation schemes. Presently, the process of flood risk modeling and management has been significantly strengthened by the collection and accessibility of high-resolution spatial information, high performing computing systems, and development in hydrological modeling methodologies. Flood danger is very dynamic with respect to space and time. The probability, size, regional extent, depth levels, and frequency of changes in the type of flood danger may be determined using the present scenarios of global climate variability. Flood risk is directly related to the geo-morphometric ranking number, and in this study it ranges from 39.18 to 55.14. Sb-4 was found to be at high flood risk with a ranking value of 55.14, whereas sb-11 was marked

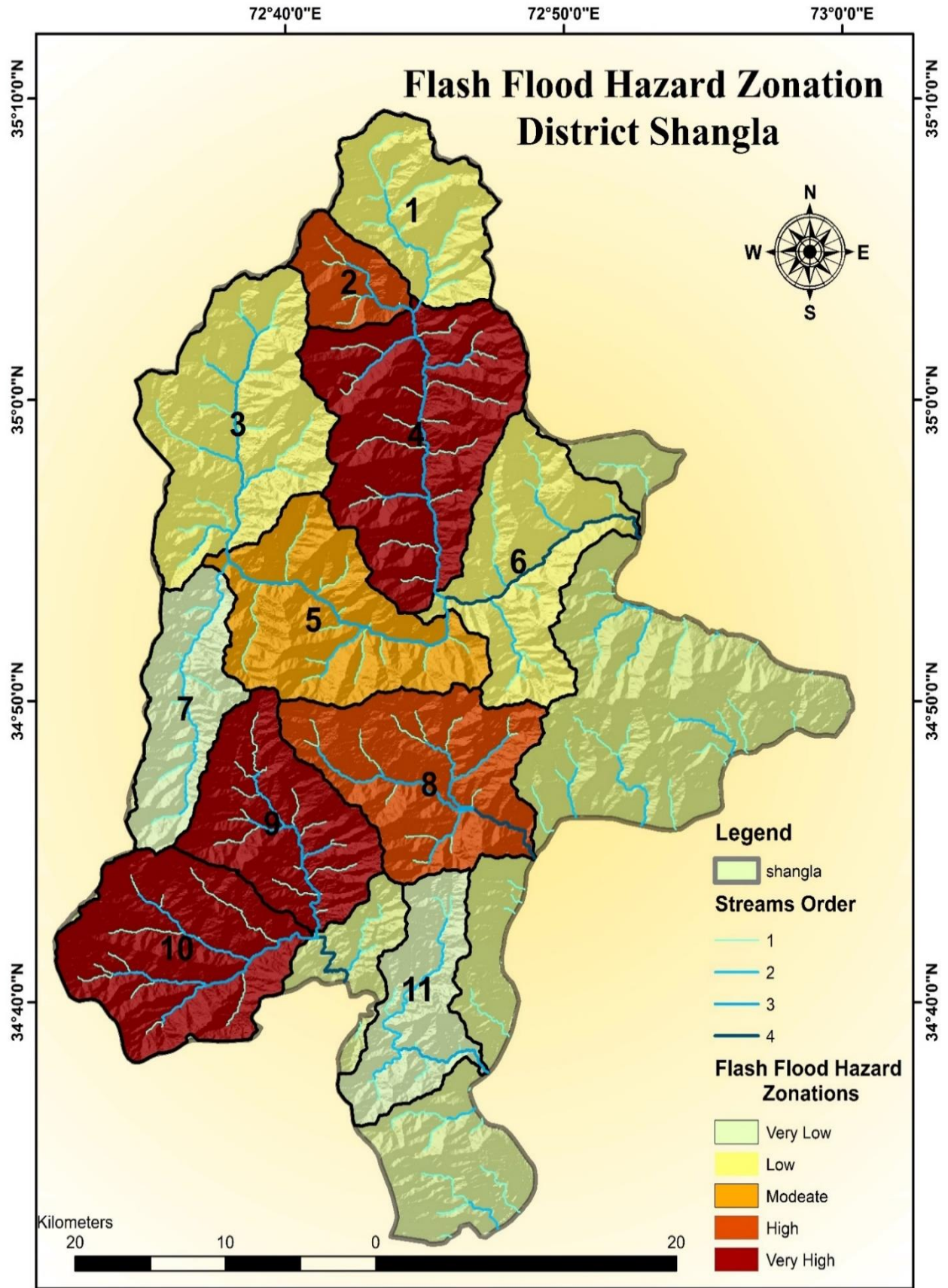


Fig. 10. Flood Hazard Zonation Map

at a very low flood risk with ranking value of 39.18. Sb-11 and sb-7 having the ranking value from 39.18 to 42.14, respectively, fall in the very low flood risk sub basins. Sb-1, sb-3 and sb-6 having ranking value 42.14 to 46.23 are in low flood risk zone. Sb-5 having ranking value 46.23 to 47.43 is in moderate flood risk. Sb-2 and sb-8 having the high flood risk with ranking value of 47.43 to 51.41, respectively. Sb-4, sb-9 and sb-10 are in the very high flood risk zones in the study area with ranking value ranging from 51.41 to 55.14. This model identifies sub-basins with very high to very low flood potential and gives spatial evaluation of hydrologic responsiveness of all sub-basins based on geo-morphometric parameters. The study concludes that primary causes of a high degree of flood hazard are the dense network of streams, high relief ratio, steep gradient, and the impermeable character of the surface rocks. The National, provincial Disaster Management Authorities and the District administration should use the outcome of this study and extend the technique to other regions.

## 6. RECOMMENDATIONS

On the basis of results derived from this study, the following are recommended;

- A long term policy should be adopted to mitigate the flash floods.
- Conservation Structures should be constructed to conserve the soil and reduce the impact of flash floods on agriculture land.
- Disaster risk reduction activities should be started on priority basis in order to reduce the human loss and livestock, and to reduce the damage of floods to physical infrastructure.

## 7. ACKNOWLEDGEMENTS

The authors would like to thank the anonymous reviewers for their critical review. The authors strongly acknowledge the support of the Secretary Agriculture Department of Khyber Pakhtunkhwa and the Director General, Soil and Water Conservation, Khyber Pakhtunkhwa, for their support throughout this study.

## 8. CONFLICT OF INTEREST

The authors declare no conflict of interest.

## 9. REFERENCES

1. V. Bain, O. Newinger, E. Gaume, P. Bernardara, M. Barbuc, and A. Bateman. *European flash floods data collation and analysis*. 273 (2009).
2. A.M. Yousaf, B. Pradhan, and S.A. Sefry. Flash flood susceptibility assessment in Jeddah city (Kingdom of Saudi Arabia) using bivariate and multivariate statistical models. *Environmental Earth Sciences* 75(1): 1-16 (2016).
3. G. Collier. Flash flood forecasting: What are the limits of predictability? *Quarterly Journal of the Royal Meteorological Society. A journal of the atmospheric sciences, applied meteorology and physical oceanography* 133.622: 3-23 (2007).
4. E. Krausmann, and F. Mushtaq. A qualitative Natech damage scale for the impact of floods on selected industrial facilities. *Natural Hazards* 46.2: 179-197 (2008).
5. R. Shaw. Floods in the Hindu Kush Region. causes and socio-economic aspects. *Mountain hazards and disaster risk reduction*. Springer, Tokyo, 33-52 (2015).
6. S. Mahmood, and S. Ullah. Assessment of 2010 flash flood causes and associated damages in Dir Valley, Khyber Pakhtunkhwa Pakistan. *International Journal of Disaster Risk Reduction* 16: 215-223 (2016).
7. M. Dawood. Impact of rainfall fluctuation on river discharge in Hindu Kush Region, Pakistan. *Abasyn Journal of Social Science* 10 :246-259 (2017).
8. H. Aksoy, V. Kirca, H.I. Burgan, and D. Kellecioglu. Hydrological and hydraulic models for determination of flood-prone and flood inundation areas. *Proceedings of the International Association of Hydrological Sciences* 373: 137-141 (2016).
9. W.Z. Kundzewicz, and J. Jania. Extreme hydro-meteorological events and their impacts. *From the global down to the regional scale*. (2007).
10. B. Mazzorana, J. Hübl, and S. Fuchs. Improving risk assessment by defining consistent and reliable system scenarios. *Natural Hazards and Earth System Sciences* 9.1: 145-159 (2009).
11. IPCC, Climate Change 2014, Synthesis Report. Contribution of Working Groups I, II and III to the Fifth Assessment Report of the Intergovernmental Panel on Climate Change [Core Writing Team, R.K. Pachauri and L.A. Meyer (eds.)]. IPCC, Geneva, Switzerland, 151 (2014).
12. S.N. Jonkman, and J. K. Vrijling. Loss of life due to floods. *Journal of Flood Risk Management* 1.1: 43-56 (2008).
13. E.M. Ibarra. A geographical approach to post-flood analysis. The extreme flood event of 12 October 2007 in Calpe (Spain). *Applied Geography* 32.2: 490-500 (2012).
14. J.D. Creutin, M. Borga, E. Grunfest, C. Lutoff, D. Zoccatelli, and I. Ruin. A space and time framework

- for analyzing human anticipation of flash floods. *Journal of Hydrology* 482: 14-24 (2013).
15. J.D. Creutin, and M. Borga. Radar hydrology modifies the monitoring of flash-flood hazard. *Hydrological processes* 17.7: 1453-1456 (2003).
  16. D. Norbiato, M. Borga, M. Sangati, F. Zanon. Regional frequency analysis of extreme precipitation in the eastern Italian Alps and the August 29, 2003 flash flood. *Journal of hydrology* 345.3-4: 149-166 (2007).
  17. H. Hu. Rainstorm flash flood risk assessment using genetic programming: a case study of risk zoning in Beijing. *Natural Hazards* 83.1: 485-500 (2016).
  18. D. Gaetano. Time-dependent changes in extreme-precipitation return-period amounts in the continental United States. *Journal of Applied Meteorology and Climatology* 48.10: 2086-2099 (2009).
  19. M.L. Botija, and M. D. Carmen. Flash floods in Catalonia: a recurrent situation. *Advances in Geosciences*, 2010, vol. 26, p. 105-111 (2010).
  20. M. Shehata, and M. Hideki. Flash flood risk assessment for Kyushu Island, Japan. *Environmental earth sciences* 77.3: 1-20 (2018).
  21. A.M. Rossa., F.L. Del Guerra, M. Borga, F. Zanon, T. Settin, and D. Leuenberger. Radar-driven high-resolution hydro-meteorological forecasts of the 26 September 2007 Venice flash flood. *Journal of Hydrology* 394.1-2 : 230-244 (2010).
  22. P.T.T. Ngo, N.D. Hoang, B. Pradhan, Q.K. Nguyen, X.T. Tran, Q.M. Nguyen, and D. Tien Bui. A novel hybrid swarm optimized multilayer neural network for spatial prediction of flash floods in tropical areas using sentinel-1 SAR imagery and geospatial data. *Sensors* 18.11: 3704. (2018).
  23. A. Arora, M. Pandey, M.A. Siddiqui, H. Hong, and V.N. Mishra. Spatial flood susceptibility prediction in Middle Ganga Plain: comparison of frequency ratio and Shannon's entropy models. *Geocarto International* 36.18: 2085-2116 (2021).
  24. W. Chen, Y. Li, W. Xue, H.shahabi, S. Li, H. hong, and B.B. Ahmad. Modeling flood susceptibility using data-driven approaches of naïve bayes tree, alternating decision tree, and random forest methods. *Science of The Total Environment* 701: 134979 (2020).
  25. M.I. Gad, A.I. El-Shiekh, and R.A. Khalifa, K.A.Ahmed. Flash flood risk assessment applying multi-criteria analysis for some northwestern coastal basins, Egypt. *European Journal of Business and Social Sciences* 4.10: 41-60 (2016).
  26. W.M. Elsadek. M.G. Ibrahim, and W. Mahmud. Flash flood risk estimation of Wadi Qena Watershed, Egypt using GIS based morphometric analysis. *Applied Environmental Research* 40.1: 36-45 (2018).
  27. K. Thakkar, and S.D. Dhiman. Morphometric analysis and prioritization of miniwatersheds in Mohr watershed, Gujarat using remote sensing and GIS techniques. *Journal of the Indian society of Remote Sensing* 35.4: 313-321 (2007).
  28. K. Martins, and B.L. Gadiga. Hydrological and morphometric analysis of upper Yedzaram catchment of Mubi in Adamawa state, Nigeria Using geographic information system (GIS). *World Environment* 5.2: 63-69 (2015).
  29. N. Mundetia, D. Sharma, and S.K. Dubey. Morphometric assessment and sub-watershed prioritization of Khari River basin in semi-arid region of Rajasthan, India. *Arabian Journal of Geosciences* 11.18: 1-18 (2018).
  30. S.K. Yadav, A. Dubey, S.K. Singh, D. Yadav. Spatial regionalisation of morphometric characteristics of mini watershed of Northern Foreland of Peninsular India. *Arabian Journal of Geosciences* 13.12: 1-16 (2020).
  31. S. Singh, S. Kanhaiya, A. Singh, and K. Chaubey. Drainage network characteristics of the Ghaghghar river basin (GRB), Son valley, India. *Geology, Ecology, and Landscapes* 3.3: 159-167 (2019).
  32. C.S. Jahan, M.F. Rahman, R.Arefin, S. Ali, and Q.H. Mazumder. Morphometric analysis and hydrological inference for water resource management in Atrai-Sib River basin, NW Bangladesh using remote sensing and GIS technique. *Journal of the Geological Society of India* 91.5: 613-620 (2018).
  33. P.P. Choudhari, G.K. Nigham, S.K. Singh, and S. Thakur. Morphometric based prioritization of watershed for groundwater potential of Mula river basin, Maharashtra, India. *Geology, Ecology, and Landscapes* 2.4: 256-267 (2018).
  34. V.P. Patil, and S.P. Mali. Watershed characterization and prioritization of Tulasi subwatershed: a geospatial approach. *Int J Innov Res Sci Eng Technol* 2.6: 2182-2189 (2013).
  35. N.A. Zaigham, O.S. Abuzirazia, G.A. Mahar, and Z.A. Nayyar. Hydrogeologic assessment for groundwater prospects in Al-Abwa drainage basin, arid-terrain of Arabian Shield, Saudi Arabian Red Sea coastal belt. *Arabian Journal of Geosciences* 13.10: 1-11 (2020).
  36. S. Mahmood, and A. Rahman. Flash flood susceptibility modeling using geo-morphometric and hydrological approaches in Panjkora Basin, Eastern Hindu Kush, Pakistan. *Environmental earth sciences* 78.1: 1-16 (2019).
  37. S. Davolio. Numerical forecast and analysis of a tropical-like cyclone in the Ionian Sea. *Natural Hazards and Earth System Sciences* 9.2: 551-562 (2009).
  38. R. Hajam, A. Hamid, and S. Bhat. Application of morphometric analysis for geo-hydrological studies

- using geo-spatial technology—a case study of Vishav Drainage Basin. *Hydrology Current Research* 4.3: 1-12 (2013).
39. T.A. Kanth, and Z. Hassan. Morphometric analysis and prioritization of watersheds for soil and water resource management in Wular catchment using geo-spatial tools. *Int J Geol Earth Environ Sci* 2.1: 30-41 (2012).
  40. G. Tarboton. A new method for the determination of flow directions and upslope areas in grid digital elevation models. *Water resources research* 33.2: 309-319. (1997)
  41. R. Parveen, U. Kumar, and V.K. Singh. Geomorphometric characterization of Upper South Koel Basin, Jharkhand: a remote sensing & GIS approach. *Journal of Water Resource and Protection* 4.12: 1042 (2012).
  42. R. Hajam, A. Hamid, and S. Bhat. Application of morphometric analysis for geo-hydrological studies using geo-spatial technology—a case study of Vishav Drainage Basin. *Hydrology Current Research* 4.3: 1-12 (2013).
  43. C. Ramu, B. Mahalingam, and P. Jayashree. Morphometric analysis of Tungabhadra drainage basin in Karnataka using geographical information system. *Journal of Electrical and Computer Engineering* 2.7: 1-7 (2013).
  44. M.L. Waikar, and A.P. Nilawar. Morphometric analysis of a drainage basin using geographical information system: a case study. *Int J Multidiscip Curr Res* 2.2014: 179-184 (2014).
  45. K. Martins, and B.L. Gadiga. Hydrological and morphometric analysis of upper Yedzaram catchment of Mubi in Adamawa state, Nigeria. Using geographic information system (GIS). *World Environment* 5.2: 63-69 (2015).
  46. R.P. Rai, K. Mohan, S. Mishra, A. Ahmad, and V.N. Mishra A GIS-based approach in drainage morphometric analysis of Kanhar River Basin, India. *Applied Water Science* 7.1: 217-232 (2017).
  47. B. Pradhan. Flood susceptible mapping and risk area delineation using logistic regression, GIS and remote sensing. *Journal of Spatial Hydrology* 9.2 (2010).
  48. S.A. Rahaman. Prioritization of sub watershed based on morphometric characteristics using fuzzy analytical hierarchy process and geographical information system—A study of Kallar Watershed, Tamil Nadu. *Aquatic Procedia* 4: 1322-1330 (2015).
  49. H. S. Aldharab, and S. A. Ali. Analysis of Basin Geometry in Ataq Region, Part of Shabwah Yemen: Using Remote Sensing and Geographic Information System Techniques. *Bulletin of Pure & Applied Sciences-Geology* 1 (2019).
  50. S. Lama, and R. Maiti. Morphometric Analysis of Chel River Basin, West Bengal, India, using Geographic Information System. *Earth Science India* 12.1 (2019).
  51. P. D. Sreedevi, P.D. Sreekanth, H.H. Khan, and S. Ahmad. Drainage morphometry and its influence on hydrology in a semi arid region: using SRTM data and GIS. *Environmental earth sciences* 70.2: 839-848 (2013).
  52. Y.I. Farhan, O. Anaba, and A. Salim. Morphometric analysis and flash floods assessment for drainage basins of the Ras En Naqb Area, South Jordan using GIS. *Applied Morphometry and Watershed Management Using RS, GIS and Multivariate Statistics (Case Studies)* 413 (2017).
  53. N. Mundetia, D. Sharma, and S.K. Dubey. Morphometric assessment and sub-watershed prioritization of Khari River basin in semi-arid region of Rajasthan, India. *Arabian Journal of Geosciences* 11.18: 1-18 (2018).
  54. S. Nag, M.B. Roy, and P.K. Roy. Optimum prioritisation of sub-watersheds based on erosion-susceptible zones through modeling and GIS techniques. *Modeling Earth Systems and Environment* 6.3: 1529-1544 (2020).
  55. B. Ahmed, and P. Sammonds. Flash flood susceptibility assessment using the parameters of drainage basin morphometry in SE Bangladesh. *Quaternary International* 575: 295-307. (2021)
  56. S.A. Mohamed, and M.E. El-Raey. Vulnerability assessment for flash floods using GIS spatial modeling and remotely sensed data in El-Arish City, North Sinai, Egypt. *Natural Hazards* 102.2: 707-728 (2020).
  57. N. Sadhasivam, A. Bhardwaj, H.R. Pourghmesmi, and N.P. Kamraj. Morphometric attributes-based soil erosion susceptibility mapping in Dnyanganga watershed of India using individual and ensemble models. *Environmental Earth Sciences* 79.14: 1-28 (2020).
  58. N.M. Ogarekpe. Flood vulnerability assessment of the upper Cross River basin using morphometric analysis. *Geomatics, Natural Hazards and Risk* 11.1: 1378-1403 (2020).
  59. V. Gardiner, and C.C. Park. Drainage basin morphometry: review and assessment. *Progress in Physical Geography* 2.1: 1-35 (1978).
  60. N. Strahler. Quantitative analysis of watershed geomorphology. *Eos, Transactions American Geophysical Union* 38.6: 913-920 (1957).
  61. S.A. Schumm. Evolution of drainage systems and slopes in badlands at Perth Amboy, New Jersey. *Geological society of America bulletin* 67.5: 597-646 (1956).
  62. Y.I. Farhan, O. Anaba, and A. Salim. Morphometric analysis and flash floods assessment for drainage basins of the Ras En Naqb Area, South Jordan Using GIS. *Journal of Geoscience and Environment Protection* 4.6: 9-33 (2016).

